J Mater Sci (2014) 49:6803–6812
DOI 10.1007/s10853-014-8382-1

Cryogenic equal channel angular pressing of commercially pure titanium: microstructure and properties

A. V. Podolskiy · H. P. Ng · I. A. Psaruk · E. D. Tabachnikova · R. Lapovok

Received: 12 March 2014 / Accepted: 4 June 2014 / Published online: 25 June 2014

Abstract Cylindrical samples of CP Titanium (Grade 2) were deformed by one, two and three passes of equal channel angular pressing (ECAP) each at temperatures 77, 300 and 575 K, respectively. The microstructure of samples processed at 77 K shows retardation of recrystallisation, high density of dislocations and deformation twins, diffuse and obscure grain boundaries compare to microstructure of samples processed at room and high temperature, where recrystallised ultrafine equiaxed grains are observed. Mechanical properties for all structural states of Ti were studied by microhardness measurements at 300 K and uniaxial compression at temperatures 300, 170, 77 and 4.2 K. Higher levels of ECAP deformation (more passes of ECAP) lead to higher values of strength and hardness at all studied temperatures. Decrease of ECAP temperature leads to increase of strength characteristics in all cases. Influence of ECAP and compression temperatures on possible changes of deformation mechanism are discussed.

A. V. Podolskiy (✉) · I. A. Psaruk · E. D. Tabachnikova
B. Verkin Institute for Low Temperature Physics & Engineering, 47, Lenin Ave, Kharkov 61103, Ukraine
e-mail: podolskiy@ilt.kharkov.ua

I. A. Psaruk
e-mail: psaruk@ilt.kharkov.ua

E. D. Tabachnikova
e-mail: tabachnikova@ilt.kharkov.ua

H. P. Ng · R. Lapovok
CAHM, Materials Engineering Department, Monash University, Clayton, VIC, Australia
e-mail: rimma.lapovok@monash.edu

Introduction

Severe plastic deformation (SPD) of different metallic materials at low temperatures has been performed by different methods such as cryogenic rolling [1, 2], multi-axial forging [3], high pressure torsion [4, 5], ECAP [6, 7], drawing [8] and others. The use of cryogenic temperatures for SPD processing is justified by suppression of dynamic recovery and enhancement of grain refinement in comparison to room temperature deformation. It is suggested that finer grains below 0.2 μm could be obtained if SPD processing performed at low temperature, and, therefore, mechanical properties such as strength and ductility could be significantly enhanced [4].

In this work, a comparative study of microstructure formation in CP Titanium (Grade 2) deformed by one, two and three passes of equal channel angular extrusion (ECAP) at temperatures 77, 300 and 575 K has been performed. The microstructure characterisation was followed by comprehensive study of mechanical properties at the range of temperatures from room temperature to 4.2 K.

Material and experimental procedures

Commercially pure titanium, CP-Ti Grade 2 (0.16 wt% of O, which corresponds to 0.48 at.%), in the form of extruded rod of 10-mm diameter was used in this work. Samples of 35-mm length were cut from the rod and dipped into liquid nitrogen. Then, the samples were dropped in the entry channel of ECAP rig and immediately pressed. The time between extracting the sample from liquid nitrogen and the end of pressing did not exceed 10 s. Our previous experimental study of thermal diffusivity of CP-Ti [9] and numerical simulations of temperature during ECAP shows

that this time is insignificant to change the temperature within the sample, except in the very thin surface layers, which are removed before microstructural or mechanical study.

Samples were subjected to one, two and three ECAP passes with cooling in the liquid nitrogen before each pass. Each pass of ECAP introduces equivalent strain in the material equal to 1.15 [10]. The ECAP rig used for processing is described elsewhere [11, 12].

The microstructures of the Ti samples ECAP processed at different conditions were examined with conventional and high-resolution (HR) transmission electron microscopy (TEM). Thin foil samples for TEM studies were prepared with a Struers Tenupol-5 twin-jet electropolisher using a solution containing 5 % perchloric acid, 35 % butoxyethanol and 60 % methanol by volume. The applied voltage and temperature of the solution were maintained at 60 V and −35 °C, respectively, during the electropolishing process.

General characterisations of the deformed Ti matrices were carried out with a FEI Tecnai G2 T20 microscope operating at 200 kV. Selected area electron diffraction (SAED) pattern of samples was obtained using an aperture size of approximately 10 μm on image. A JOEL 2100F FEG microscope operating at 200kV was employed to record HRTEM images of the defect structures within the grains.

Electron backscatter diffraction (EBSD) analysis was carried out on electropolished samples. Crystallographic data were analysed with a FEI Quanta 3D FEG scanning electron microscope (SEM) incorporating a TSL OIM^{TM} system.

For the measurement of the Vickers microhardness, samples were prepared by spark erosion, grinding and polishing from transversal (perpendicular to the extrusion direction) sections, the applied load was 2.0 N for 10 s, and the indentations were applied in intervals of 0.2 mm along 4 different radial directions from the centre to the edge of sample.

Compression samples of square 1.8×1.8 mm^2 cross section and height of 3.5 mm were cut from ECAP billets and also from initial coarse-grained (CG) Ti rod by spark erosion with the height parallel to extrusion direction. The mechanical characteristics of ECAP processed as well as of coarse-grained Ti samples were studied by recording the load–displacement curves during compression with a strain rate 3×10^{-4} s^{-1} in an MRK-3 deformation machine at ambient temperature of 300 K and cryogenic temperatures achieved with liquid nitrogen and helium. The load–displacement data were converted into engineering stress–strain curves $\sigma(\varepsilon)$ relevant to initial dimensions of the sample.

During the measurement of the deformation curves in some samples, the shear flow stress sensitivity $\Delta\tau/\Delta\ln\dot{\varepsilon}_a$ was measured by increasing the rate of deformation from $\dot{\varepsilon} = 3 \times 10^{-4}$ s^{-1} by a factor of 6.6. The shear stress τ was expressed as $\tau = 0.5\ \sigma$ [13]. For construction the temperature dependence of the shear flow stress sensitivity, the $\Delta\tau/\Delta\ln\dot{\varepsilon}$ values were used at $\varepsilon = 2$ %.

According to the standard formula [14], the values of activation volume for the process of plastic deformation were calculated from the rate sensitivity of flow stress

$$V(T) = kT\frac{\Delta\ln\dot{\varepsilon}}{\Delta\tau(T)}, \quad (1)$$

where k is the Boltzmann constant.

Experimental results

Microstructure characterisation

The bright-field (BF) electron images and the corresponding SAED patterns of the CP-Ti samples ECAP processed under different temperatures, T, and number of passes, N, are summarised in Fig. 1.

Comparing the microstructures processed at the cryogenic temperature, i.e. 77 K, there exists an obvious trend that the density of strain contours (dark bands) in matrix grains increases significantly with the number of passes, see Fig. 1a, d, g for $N = 1$, 2 and 3, respectively. The strain contours are diffraction contrasts caused by the rotation of the lattice planes, and thus their density reflects the magnitude of the residual stress fields. Detailed microscopic examinations of the specimen processed at $T = 77$ K for $N = 1$ revealed a highly dislocated matrix, but no apparent dislocation cell structures could be observed therein. Well-defined cell structures or subgrains only became visible in specimens processed with $N = 2$ or above. The development of highly misoriented cells or subgrains in the specimen processed at $T = 77$ K for $N = 3$ is evidenced by the occurrence of continuous diffraction rings (or ring segments) in its corresponding SAED pattern, Fig. 1g. The presence of zone-axis type reflection maxima in the SAED pattern suggests that a substantial portion of the parent grain remains unrefined even after 3 ECAP passes at the cryogenic temperature.

An increase of the ECAP temperature to 300 K led to considerable formation of low-angle grain boundaries in the sample processed with one pass ($N = 1$), which are inferred by the streaked diffraction spots in Fig. 1b. This plausibly suggests that subgrains having low misorientations were developed in the matrix. An increase in number of ECAP passes to $N = 2$ at the same temperature resulted in an extended formation of subgrains within the primary grain. These subgrains, arranged preferentially in cluster forms, are manifested by the regions of mottled contrast

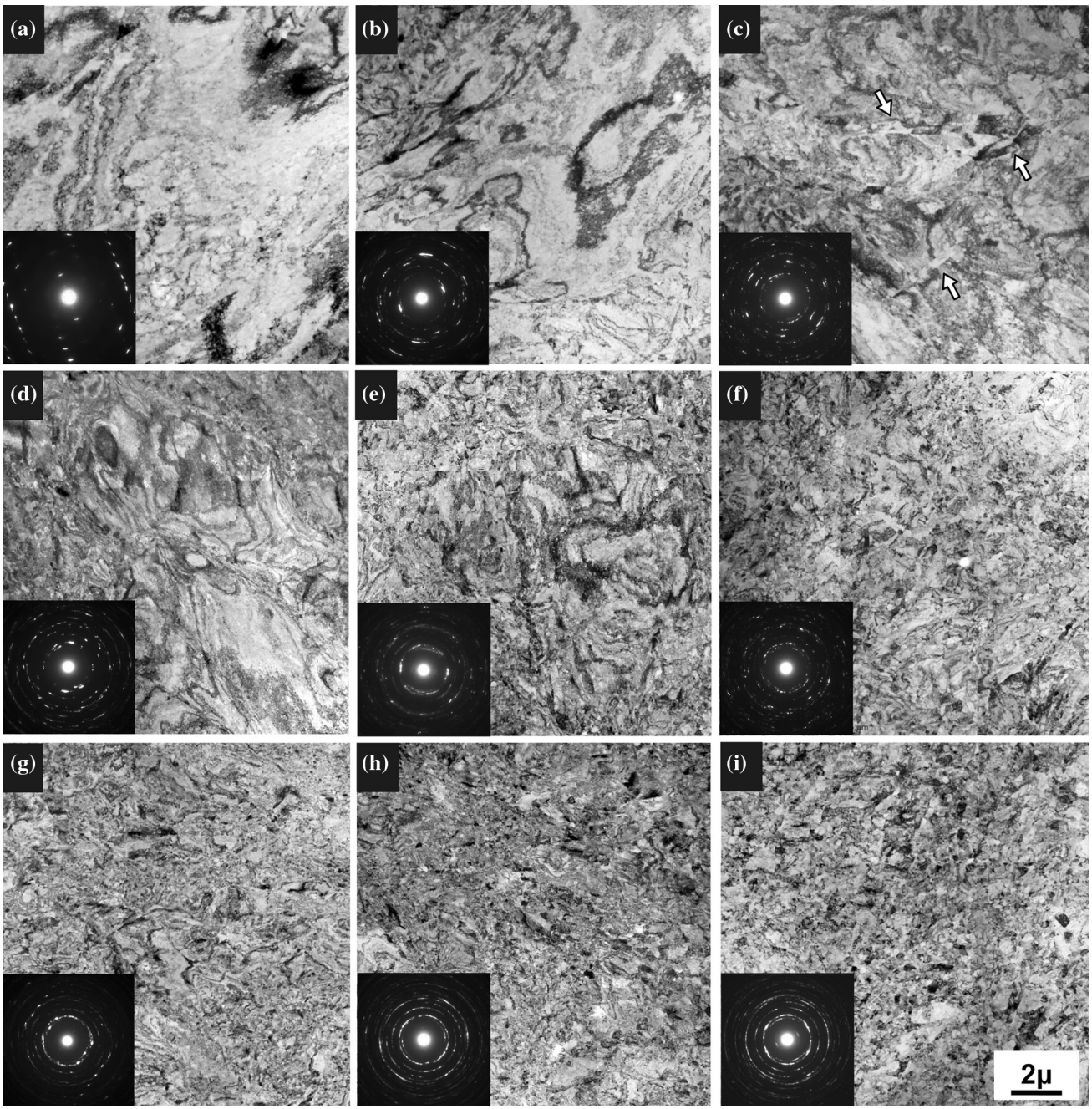

Fig. 1 Representative microstructures of the CP-Ti samples processed under different ECAP conditions: **a** 1 pass at 77 K, **b** 1 pass at 300 K, **c** 1 pass at 575 K, **d** 2 passes at 77 K, **e** 2 passes at 300 K, **f** 2 passes at 575 K, **g** 3 passes at 77 K, **h** 3 passes at 300 K and **i** 3 passes at 575 K. *Inset* in each figure represents the corresponding electron diffraction patterns

having a sub-micron size-scale in the BF image, Fig. 1e. Further ECAP deformation by three passes resulted in a relatively more homogeneous microstructure consisting of very fine subgrains having low to moderate degrees of misorientation with one another, Fig. 1h.

ECAP processing at the elevated temperature of 575 K gave rise to a considerable change in microstructures compared with the lower temperature counterparts. Figure 1c indicates that an abundance of high-angle grain boundaries has emerged in the matrix upon a single ECAP pass ($N = 1$), most of which were found to be associated with lamella grains having a longer dimension of up to several μm (e.g. the grains marked by arrows). Such an evolution in microstructure is attributable to recrystallization process which occurs more readily at elevated temperatures. It is noted that further increase in N caused the

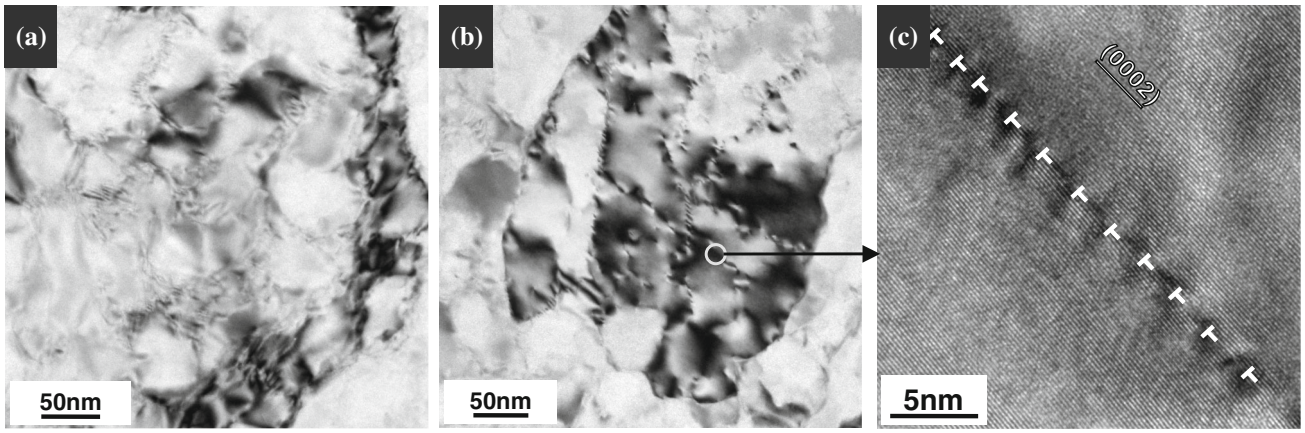

Fig. 2 Typical defect structures inside the coarse grains of the Ti samples processed with room temperature and cryogenic ECAP: BF-TEM micrographs showing nano-scale cell structures developed after 2 ECAP passes at 300 K (**a**) and 77 K (**b**), respectively, and a HRTEM micrograph showing the configuration of dislocations at the cell boundaries (**c**)

lamella grains to break down into smaller, more equiaxed ultrafine grains, see Fig. 1f, i. The result of dark-field grain size analysis (>300 grains) indicated that the sample processed at $T = 575$ K for $N = 3$ contains a distribution of recrystallized ultrafine grains having an average size of around 219 nm.

The essential difference in the dislocation substructure and cells formation at cryogenic ($T = 77$ K) and room temperature ($T = 300$ K) was confirmed by TEM study of the microstructures at high magnification after two ECAP passes, Fig. 2. The microstructure after ECAP processing at 300 K revealed the formation of dislocation cells characterised by a non-homogeneous size distribution ranging from ~10 to 80 nm. In particular, the cells walls (~10 nm in thickness) tend to exhibit a complex diffraction contrast due presumably to concentration of entangled dislocations, Fig. 2a. Conversely, a more homogenous cell size of ~50 nm in diameter was observed after the same number of ECAP passes ($N = 2$) at 77 K, Fig. 2b. The high-resolution phase-contrast image analysis revealed that the cell walls were essentially low-angle tilt boundaries each constituted by a sequence of edge dislocations, Fig. 2c.

Upon further ECAP processing to $N = 3$ at 77 K, some extremely fine crystallites (<100 nm) were noted to form in the matrix of the sample processed at 77 K. The boundaries associated with these crystallites are mostly of high misorientations. However, they are not well defined in profile but rather obscure and serrated, see Fig. 3a. It remains questionable whether these boundaries would possess distinctly different properties from the equilibrium grain boundary counterparts. By comparison, Fig. 3b shows the ultrafine grains that are typical of the sample processed at $T = 575$ K for $N = 3$. The interior of the grains is mainly free of dislocations due presumably to dynamic recovery. Although cell structures still exist in this sample, they were observed only in those heavily-deformed matrix grains that were not fully recrystallised. It is believed that the contrasting differences in the nano-scale structures resulted from these two temperatures (77 vs 575 K) would lead to dissimilar mechanical properties of their bulk materials.

In contrast to its profound effect on the size-scale of the Ti grains, EBSD analyses reveal that ECAP temperature has a relatively small influence on the texture development of the Ti matrices even when the number of ECAP passes accumulates. Figure 4a, b compares the IPF maps and the corresponding pole figures of the Ti samples processed with one ECAP pass at 77 and 575 K, respectively. Due to the circular geometry of the 3 mm disc samples used in this EBSD study, reference directions are not defined on the pole figures.

It can be seen from both sets of {0001} pole figures that poles of high intensities (Max = 10.22 for 77 K and Max = 12.22 for 575 K) are concentrated in discreet zones which correspond to a titling angle ranging from 60 to 90° with respect to the normal direction. Such a crystallographic texture is likely to be inherited from the prior texture of the raw α-Ti extruded rods which commonly exhibit the so-called 'cylindrical texture' where c-axes tend to align perpendicular to the extrusion axis. A minor but noticeable difference between these two sets of texture plots is that the sample processed at 575 K shows less intense $\langle 10\bar{1}0 \rangle$ and $\langle 11\bar{2}0 \rangle$ poles aligned with normal direction than does the 77 K counterpart.

As the number of ECAP passes increases, the texture analysis is complicated by the severe deformation of the cryogenically processed samples. Figure 4c shows the IPF map of the sample ECAP processed at 77 K for three passes. A significant portion of the matrix was not readily indexed due plausibly to the presence of an extremely high density of dislocations. The pole figures reflect the textures of the remnant grains, which may not be representative of

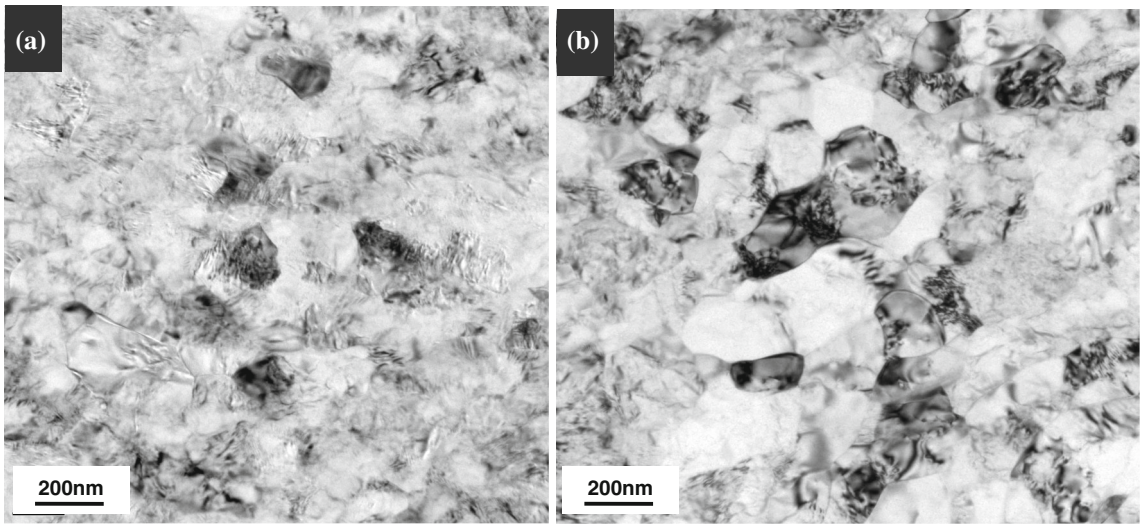

Fig. 3 Ultrafine microstructures in the Ti samples processed with ECAP at temperatures of **a** 77 K and **b** 575 K, for 3 passes

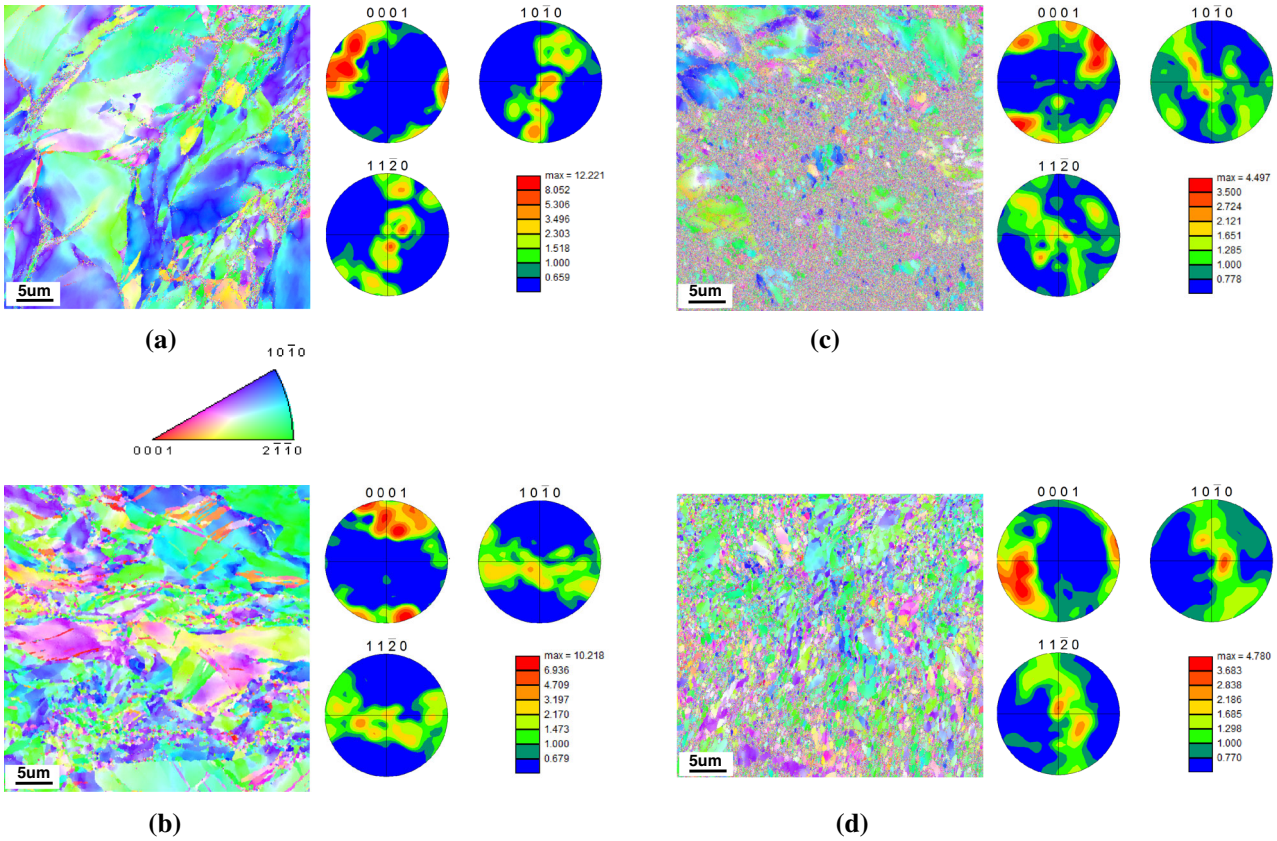

Fig. 4 IPF maps and pole figures of the ECAP-processed Ti samples: **a** 1 pass at 77 K, CI 0.45; **b** 1 pass at 575 K, CI 0.48; **c** 3 passes at 77 K, CI 0.10 and **d** 3 passes at 575 K, CI 0.28. CI refers to the average confidence index of the EBSD pattern

the entire matrix. On the other hand, Fig. 4d clearly shows that the sample ECAP processed at 575 K for three passes underwent extensive dynamic recrystallisation, resulting in the formation of sub-micron grains having a size of the order of 100 nm, in accord with the TEM observations. Albeit the high degree of recrystallisation, it is apparent that the texture of the recrystallised Ti matrix remains similar to those of the sample processed with 1 ECAP pass, cf. Fig. 4a, b, albeit that the intensity of the poles is substantially lower (Max = 4.78).

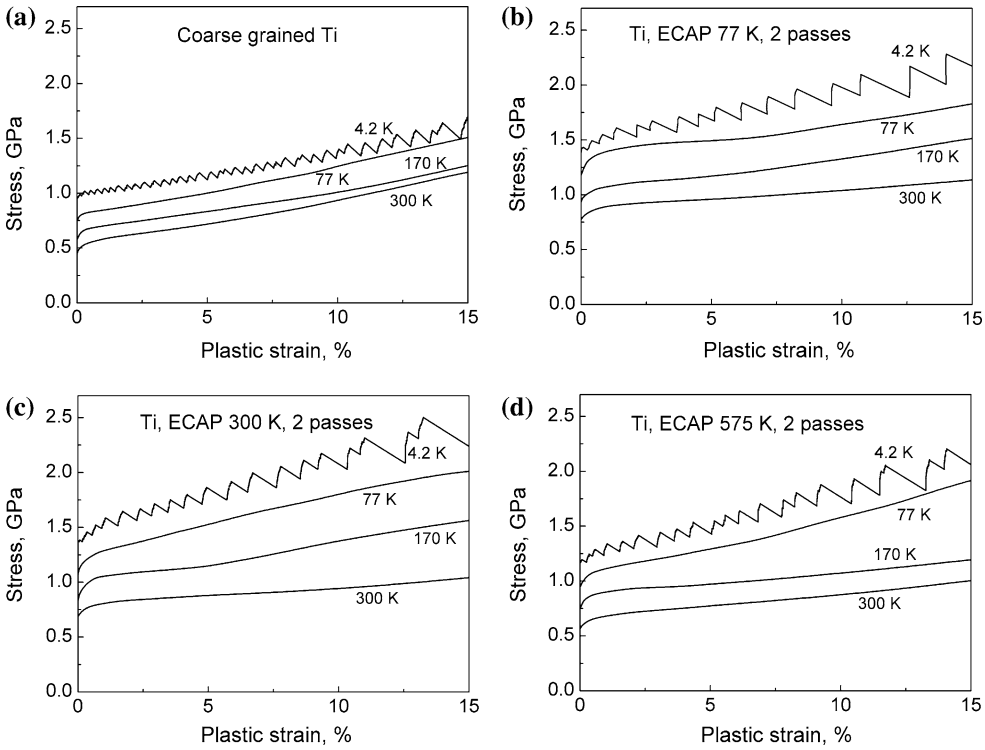

Fig. 5 Typical stress–strain curves at different compression temperatures for initial coarse-grained and ultrafine-grained (2 passes of ECAP at temperatures 77, 300, 575 K) Ti

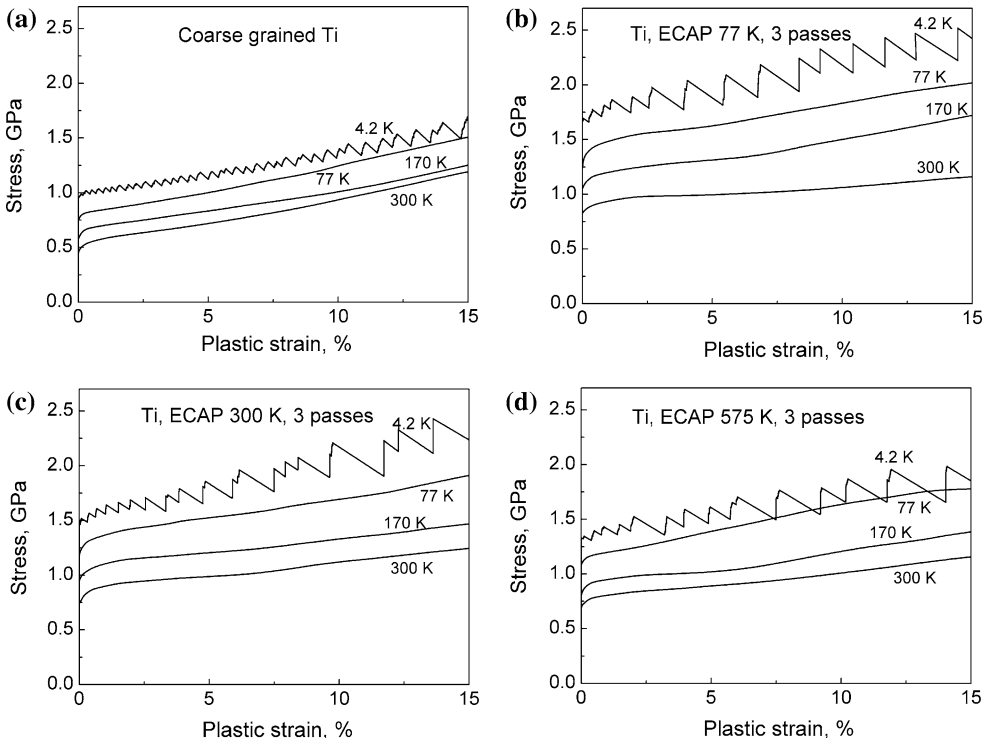

Fig. 6 Typical stress–strain curves at different compression temperatures for initial coarse-grained and ultrafine-grained (3 passes of ECAP at temperatures 77, 300, 575 K) Ti

Mechanical properties

Typical strain curves obtained in uniaxial compression at different temperatures of initial coarse-grained and ultrafine-grained Ti, which was processed by 2 and 3 passes of ECAP at temperatures 77, 300, 575 K, are shown in Figs. 5 and 6. These figures show clearly the contrast between smooth plastic flow at all moderately low temperatures and serrated plastic flow at temperature of 4.2 K. This serrated flow is typical at such low temperature of many metals and

alloys including coarse-grained Ti [15, 16], and can be explained by localisation of plastic deformation and collective and interrelated avalanche type motion of carriers of plasticity. The amplitude of serrations is considerably larger in ultrafine-grained Ti in comparison with coarse-grained structural state indicating larger concentration of barriers for carriers of plasticity in the ultrafine-grained states.

The strain curves (Figs. 5, 6) exhibit two different stages: initial 'parabolic' stage is changed at plastic strain values of 0.2–3 % by extended nearly linear region. Increase of the deforming stress at the 'parabolic' stage corresponds to increase of quantity of grains involved in process of plastic deformation, and transition to the linear stage corresponds to spreading of the plastic deformation over all grains and beginning of stable plastic flow [17, 18]. Transition to the linear stage takes place at lower values of plastic strain in coarse-grained Ti (at about 0.5 %) whilst in ultrafine-grained Ti at about 1–3 %. This indicates bi-modal distribution of grains in ultrafine-grained Ti (Fig. 4) and presence of nanograins with the size of below 100 nm, which require especially high stresses for plastic deformation.

Considerable ductility is registered for all studied structural states of Ti (more than 15 % at compression temperature of 4.2 K and more than 25 % at higher temperatures).

Severe plastic deformation by ECAP leads to significant decrease of grain size in comparison with initial coarse-grained state and correspondent increase of the material strength, clearly observed in Figs. 5 and 6. This effect seems even more pronounced in Fig. 7, where values of the yield stress are plotted for all studied structural states and compression temperatures.

It can be seen from Fig. 7 that higher level of strain (more passes of ECAP) leads to higher values of strength at all studied temperatures. Decrease of ECAP temperature leads to increase of strength characteristics in all cases: yield stress after ECAP at 300 K is approximately 10–15 % higher than after ECAP at 575 K for all studied compression temperatures. ECAP at 77 K gives additional 5–10 % increase of strength relatively to ECAP at 300 K. Similar tendency is proven by microhardness measurements for all studied structural states of Ti (Table 1).

The yield stress is increased for all studied structural states by about 70–110 % when temperature of compression decreased from room temperature to 4.2 K (Fig. 7) indicating the thermoactivated type of plastic deformation. Dependence of activation volume of plastic deformation on grain size can be identified from Fig. 8.

It can be seen from Fig. 8 that decrease of ECAP temperature and increase of ECAP passes lead to decrease of the activation volume values at all studied compression temperatures. Two ECAP passes at 575 K give nearly the same the activation volume as coarse-grained Ti indicating identical deformation mechanisms, whilst activation volume after three ECAP passes at 77 K considerably differs from coarse-grained state indicating significant change of distance between the barriers for carriers of plasticity or even change of plastic deformation mechanism. All other studied structural states are between these two limiting

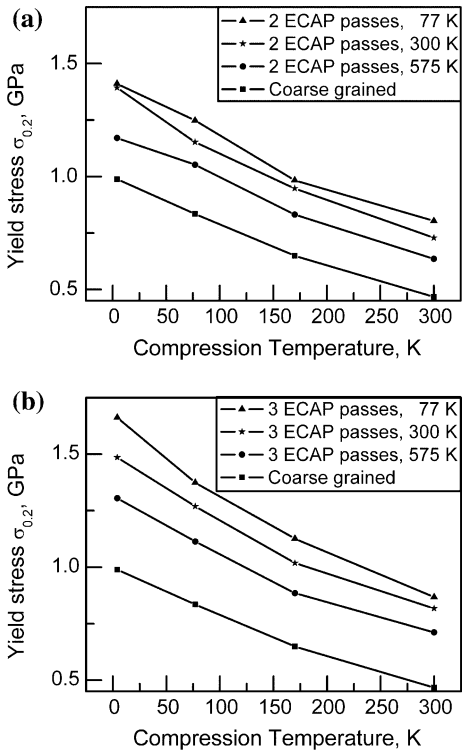

Fig. 7 Temperature dependence of yield stress in compression for coarse-grained and ultrafine-grained Ti, processed by 2 passes of ECAP at 77, 300, 575 K (**a**) and 3 passes of ECAP at 77, 300, 575 K (**b**)

Table 1 Microhardness of initial coarse-grained Ti and ultrafine-grained Ti (after 1, 2, 3 passes of ECAP at temperatures of 575, 300, 77 K)

Number of ECAP passes	ECAP temperature (K)	Vickers microhardness (GPa)
0 (initial coarse-grained state)	–	2.08
1	575	2.44
1	300	2.67
1	77	2.77
2	575	2.39
2	300	2.73
2	77	2.69
3	575	2.39
3	300	2.92
3	77	3.02

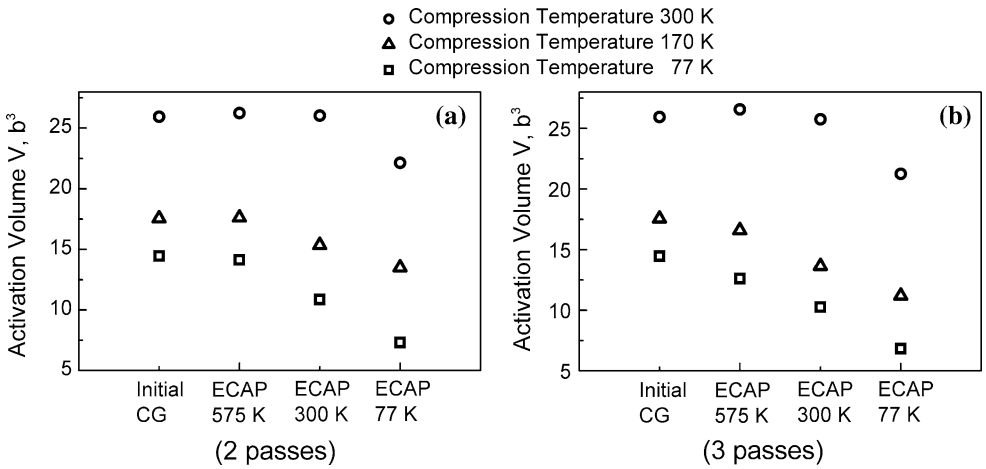

Fig. 8 Activation volume of the plastic deformation, measured at 2 % of plastic deformation in compression tests at temperatures of 77, 170, 300 K for initial coarse-grained (CG) and ultrafine-grained Ti, processed by **a** 2 and **b** 3 passes of ECAP at 575, 300, 77 K

cases, showing gradual change in activation volume (plasticity mechanisms).

Discussion of results

The microscopic mechanisms controlling the plastic deformation of coarse-grained Ti are established quite well by now. In the studied temperature range (below 300 K), the kinetic of plastic strain in CP coarse-grained Ti is controlled by thermally activated motion of dislocations over the local barriers formed by interstitial impurity atoms, mainly O and C [13]. Therefore, the dislocations in grain interium are mostly pinned at the impurity atoms, and dislocation segments between the pinning points are curved by the deforming stress. Dislocations repeatedly overcome these local barriers by thermal activation and start to move to be pinned by the next set of pinning points. The effective energy (enthalpy) of activation in this case is often used in the form [19]:

$$H(\tau*) = H_0\left[1 - \left(\frac{\tau*}{\tau_c}\right)^p\right]^q,\ 0 \le p \le 1,\ 1 \le q \le 2. \qquad (2)$$

Here, H_0 is the energy parameter of dislocation-impurity interaction; $\tau^* = \tau - \tau_i$ is effective stress, which is the difference between shear stress $\tau = 0.5\ \sigma$ and long-range internal stress τ_i; τ_c is critical stress of unactivated overcoming of local barrier by dislocation; p and q—numeric parameters.

Temperature dependences of the deforming shear stress and the activation volume can be expressed as [13, 18]

$$\tau(T) = \tau_i + \tau_c\left[1 - \left(\frac{T}{T_0}\right)^{1/q}\right]^{1/p}, \qquad (3)$$

$$V(T) = \frac{pqH_0T}{\tau_cT_0}\left(\frac{T}{T_0}\right)^{-1/q}\left[1 - \left(\frac{T}{T_0}\right)^{1/q}\right]^{(p-1)/p}. \qquad (4)$$

Empirical values of the parameters p, q, H_0, T_0, τ_c for Ti with different contents of O can be found in [13]. It should be also noted that decrease of average distance between the local barriers for dislocation motion in Ti (increase of impurity concentration) leads to increase of stress values and to decrease of activation volume for all studied impurity concentration range [13]. Average length of the dislocation segment between the pinning points in coarse-grained Ti can be written as [13]

$$L = \beta bC^{-1/2}, \qquad (5)$$

where C is atomic concentration of oxygen; β is empirical parameter ($\beta \approx 3$).

Values and temperature dependences of the yield stress and the activation volume of the coarse-grained Ti (Figs. 7, 8) can be described by relations (3) and (4). Two ECAP passes at 575 K lead to formation of submicron grains in Ti, to decrease of average grain size in comparison with initial coarse-grained Ti and corresponding to considerable increase of yield stress at all studied compression temperatures (Figs. 5, 7). Whilst values of the activation volume are practically identical for these two structural states, which indicate that mechanism of plastic deformation after such ECAP treatment is also the thermally activated overcoming of the impurity atoms. Decrease of the grain size in this case does not lead to change of the average length of the dislocation segment L, which can be estimated using relation (5) taking in account the atomic concentration of O in Ti (0.0048) as $L \approx 43$ b, i.e. distance between the pinning points is considerably smaller than grain sizes, and grain boundaries cannot affect significantly the average dislocation segment length. Changes of grain size mainly cause change of level of internal stresses τ_i (Eq. 3) and correspondently the value of deforming stress. If the grain size decreased down to the dislocation segment length, the grain boundaries would not be acting as the additional pinning points for dislocations.

In this case, the grain boundaries appear to be the strong barriers for dislocations, which cannot be overcome by thermal activation, and the change of deformation mechanism is expected. Decrease of ECAP temperature leads to diminished dynamic recovery [20, 21], which gives more active accumulation of defects within grains, and to lower level of recrystallization (Figs. 1, 3), resulting is smaller grain sizes and higher strength values after ECAP. Another reason for smaller grains formation and higher strength after ECAP at lower temperatures is formation of twins, which is known to be active in Ti at low temperatures [22]. Considering that twin boundaries as well as the grain boundaries are effective barriers for dislocations, an increase of twin quantity leads to increase of strength.

After 1 pass of ECAP at 77 K, the overwhelming part of the Ti volume remained coarse grained (Figs. 1a, 4a), whilst strength and hardness of this structural state are considerably higher in comparison with initial coarse grained and material after 1 pass of ECAPed at 300 and 575 K. It can be explained by formation of rather thin layers of nanosized grains (cells) around the coarse grains in this structural state (Fig. 4a); these layers can be efficient barriers for dislocation motion, which leads to increase of strength. 1 ECAP pass at higher temperatures gives more efficient grain refinement—larger quantity of fragmented grains is observed (Fig. 1, 4) in comparison with material after 1 ECAP pass at 77 K, but typical size of these fragments of the grains is larger in comparison with nanosized grains after ECAP at 77 K. Higher level of severe plastic deformation (2 and 3 ECAP passes at 77 K) leads to formation of more developed ultrafine-grained structures with minor portion of remnant coarse grains embedded in ultrafine-grained matrix (Figs. 1, 4c) and increase of hardness (strength). At higher ECAP temperatures, smaller quantity of the remnant coarse grains can be observed, whilst ultrafine-grained subsystem has average sizes larger in comparison with ECAP at 77 K (Fig. 4c, d), resulting in lower strength. Moreover, the grain boundaries of recrystallized grains with r low energy formed after ECAP at 300 and 575 K are easier to penetrate by dislocations in comparison with not recrystallized grains after ECAP at 77 K, which also explains observed higher strength at low ECAP temperature.

Decrease of the activation volume of plastic deformation is observed with decrease of ECAP temperature (Fig. 8). At compression temperature of 300 K, the decrease of activation volume starts in the structural state of Ti, produced by ECAP at lowest temperature (77 K), whilst at lower compression temperatures, changes of activation volume start at higher ECAP temperatures (300 and 575 K). After 3 ECAP passes, changes of activation volume are more pronounced in comparison with two ECAP passes. Two explanations of these observed changes of the activation volume are suggested:

(i) Decrease of ECAP temperature and/or increase of the number of ECAP passes lead to increase of defects (dislocations, forest of dislocations, subgrain boundaries, etc.) in grains due to suppressed dynamic recovery at lower ECAP temperatures. When the distance between these defects becomes comparable with the distance between the impurity atoms, the number of efficient pinning points for dislocations considerably increases and the average length of the dislocation segments between the pinning points and the values of the activation volume decreases;
(ii) Decrease of the ECAP temperature and/or increase of number of ECAP passes lead to decrease in average grain size, which triggers the change of deformation mechanisms at sufficiently small grain sizes [23].The concentration of oxygen does not control any more the process of plastic deformation in ultrafine-grained Ti.

The effect similar to (i) was observed for coarse-grained Ti with different concentrations of oxygen [13]. It was observed that increase of oxygen concentration leads to increase of the number of pinning points for dislocations, and decrease of average dislocation segment length, which results in increase of the strain rate sensitivity (decrease of activation volume). For different oxygen concentrations [13], the biggest difference of the strain rate sensitivity (activation volume) was observed near 300 K, which decreased proportionally with decrease of strain temperature. However, in our case, the difference in activation volume for different structural states increases with decreasing of strain temperature. This indicates that change of average distance between the pinning points (i) apparently does not determine the observed changes of the activation volume (Fig. 8), and the more plausible explanation of these changes is the change of the deformation mechanism triggered by decrease of ECAP temperature and increase of the number of ECAP passes. The values of the activation volume for different structural states of Ti and different strain temperatures (Fig. 8) can be considered as a kind of map of deformation mechanisms, which clearly indicates the temperatures and grain sizes where the change of the deformation mechanism starts. The available experimental data do not identify in which specific deformation mechanism controls the plastic deformation of ultrafine-grained Ti, but it can be speculated that nucleation of dislocations at grain boundaries is the dominant one as widely discussed in the literature [24].

Conclusions

The results of this work can be summarised as follows:

- 1 and 2 ECAP passes produce complex structures, whereas areas of ultrafine grains coexist with remaining large grains.
- ECAP at 575 and 300 K results in rather equiaxed grains with clear grain boundaries due to action of the dynamic recovery, whilst ECAP at 77 K leads to diffuse and obscure grain boundaries;
- 3 ECAP passes result in more uniform microstructures with smaller average grain sizes;
- Decrease of ECAP temperature and increase of level of severe plastic deformation lead to higher strength characteristics in all studied cases: yield strength after ECAP at 300 K is approximately 10–15 % higher in comparison with ECAP at 575 K for all studied compression temperatures. ECAP at 77 K gives additional 5–10 % increase of strength in comparison with ECAP at 300 K;
- High ductility is registered for all studied structural states and compression temperatures;
- Considerable increase of strength with decrease of compression temperature indicates the thermoactivated plastic deformation;
- Thermoactivated motion of dislocations over local barriers (impurity atoms) in grains is the microscopic mechanism of plastic deformation of coarse-grained Ti and ultrafine-grained Ti processed by ECAP at higher temperatures.
- Decrease of ECAP temperature and increase of the number of ECAP passes lead to the change of the deformation mechanism, which can be defined from the values of the activation volume of plastic deformation for all studied structural states.

References

1. Nam WJ, Lee YB, Dong DH (2004) Ultrafine grained bulk 5083 Al alloy produced by cryogenic rolling process. Mater Sci Forum 449–452:141–144
2. Moskalenko VA, Smirnov AR, Moskalenko AV (2009) Nanocrystalline titanium produced by the cryomechanical method: microstructure and mechanical properties. Low Temp Phys 35:1160–1164
3. Yin J, Lu J, Zhang P (2004) Nanostructural formation of fine grained aluminum alloy by severe plastic deformation at cryogenic temperature. J Mater Sci 39:2851–2854. doi:10.1023/B:JMSC.0000021463.83899.b3
4. Kon'kova TN, Mironov SY, Korznikov AV (2010) Severe cryogenic deformation of copper. Phys Metal Metallogr 109:171–176
5. Podolskiy AV, Mangler C, Schafler E, Tabachnikova ED, Zehetbauer MJ (2013) Microstructure and mechanical properties of high purity nanostructured titanium processed by high pressure torsion at temperatures 300 and 77 K. J Mater Sci 48:4689–4697. doi:10.1007/s10853-013-7276-y
6. Chen YJ, Roven HJ, Gireesh SS, Skaret P, Hjelen J (2011) Quantitative study of grain refinement in Al–Mg alloy processed by equal channel angular pressing at cryogenic temperature. Mater Lett 65:3472–3475
7. Fritsch S, Scholze M, Wagner MF-X (2012) Cryogenic forming of AA7075 by equal-channel angular pressing. Mater Werkst 43:561–566
8. Kutniy KV, Volchok OI, Kislyak IF, Tikhonovsky MA, Storozhilov GE (2011) Obtaining of pure nanostructured titanium for medicine by severe deformation at cryogenic temperatures. Mater. Werkst. 42:114–117
9. Lapovok R, Molotnikov A, Levin Y, Bandaranayake A, Estrin Y (2012) Machining of course grained and ultrafine grained titanium. J Mater Sci 47:4589–4594. doi:10.1007/s10853-012-6320-7
10. Segal VM (1995) Materials processing by simple shear. Mater Sci Eng A 197:157–164
11. Lapovok R, Tomus D, Muddle BC (2008) Low-temperature compaction of Ti–6Al–4V powder using equal channel angular extrusion with back-pressure. Mater Sci Eng A 490:171–180
12. Lapovok R, Estrin Y, Popov MV, Langdon TG (2008) Enhanced superplasticity in a magnesium alloy processed by equal-channel angular pressing with a back-pressure. Adv Eng Mater 10:429–433
13. Kovaleva VN, Moskalenko VA, Natsik VD (1994) Barrier parameters and statistics controlling the plasticity of Ti–O solid solutions in the temperature range 20–550 K. Phil Mag A 70:423–438
14. Evans A, Rawlings R (1969) The thermally activated deformation of crystalline materials. Phys Stat Solidi 34:9–31
15. Pustovalov VV (2008) Serrated deformation of metals and alloys at low temperatures. Low Temp Phys 34:683–723
16. Tabachnikova ED, Bengus VZ, Podolskiy AV, Smirnov SN, Gunderov DV, Valiev RZ (2006) Low temperature mechanical properties of different commercial purity nanostructured titanium processed by ECA pressing. Mater Sci Forum 503–504:633–638
17. Li L, Anderson PM, Lee MG, Bitzck E, Derlet P, Swygenhoven HV (2009) The stress-strain response of nanocrystalline metals: a quantized crystal plasticity approach. Acta Mater 57:812–822
18. Tabachnikova ED, Podolskiy AV, Smirnov SN, Psaruk IA, Bengus VZ, Li H, Li L, Chu H, Liao PK (2012) Thermal activation plasticity of nanocrystalline Ni-18.75 at.% Fe alloy in temperature range 4.2–350 K. Low Temp Phys 38:239–247
19. Kocks F, Argon AS, Ashby MF (1975) Thermodynamics and kinetics of slip. Progr Mater Sci 19:1–288
20. Zehetbauer MJ, Zhu YT (eds) (2009) Bulk nanostructured materials. Wiley, Weinheim
21. Wang Y, Ma E (2004) Three strategies to achieve uniform tensile deformation in a nanostructured metal. Acta Mater 52:1699–1709
22. Zwicker U (1974) Titan und Titanlegierungen. Springer, Berlin
23. Meyers MA, Mishra A, Benson DJ (2006) Mechanical properties of nanocrystalline materials. Progr Mater Sci 51:427–556
24. Asaro J, Suresh S (2005) Mechanistic models for the activation volume and rate sensitivity in metals with nanocrystalline grains and nano-scale twins. Acta Mater 53:3369–3382